UMT Artificial Intelligence Review (UMT-AIR)
Volume 5 Issue 2, Fall 2025
ISSN$_{(P)}$: 2791-1276, ISSN$_{(E)}$: 2791-1268
Homepage: https://journals.umt.edu.pk/index.php/UMT-AIR

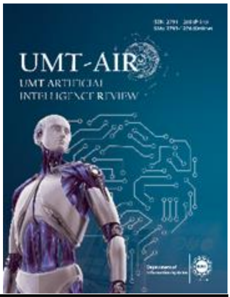

Title:	**Robust Hybrid Model for Vitiligo Skin Lesion Detection: Integrating Grey Wolf and Particle Swarm Optimization for Enhanced Feature Extraction and Classification**
Author (s):	Shardha Nand[1], Asif Raza[1], Usman Amjad[2], and Nancy Alias Shivani Kumari[3]
Affiliation (s):	[1]Sir Syed University of Engineering and Technology, Karachi, Pakistan [2]NED University of Engineering and Technology, Karachi, Pakistan [3]Sindh Madressatul Islam University, Karachi, Pakistan
DOI:	https://doi.org/10.32350.umt-air.52.03
History:	Received: July 24, 2025, Revised: October 17, 2025, Accepted: November 17, 2025, Published: December 08, 2025
Citation:	S. Nand, A. Raza, U. Amjad and N. A. S. Kumari, "Robust hybrid model for vitiligo skin lesion detection: Integrating grey wolf and particle swarm optimization for enhanced feature extraction and classification," *UMT Artif. Intell. Rev.*, vol. 5, no. 2, pp. 41–60, Dec. 2025, doi: https://doi.org/10.32350.umt-air.52.03.
Copyright:	
Licensing:	
Conflict of Interest:	Author(s) declared no conflict of interest

A publication of
Department of Information System, Dr. Hasan Murad School of Management
University of Management and Technology, Lahore, Pakistan

Robust Hybrid Model for Vitiligo Skin Lesion Detection: Integrating Grey Wolf and Particle Swarm Optimization for Enhanced Feature Extraction and Classification

Shardha Nand[1*], Asif Raza[1], Usman Amjad[2], and Nancy Alias Shivani Kumari[3]

[1]Department of Computer Science & Information Technology, Sir Syed University of Engineering & Technology, Karachi, Pakistan
[2]Department of Computer Science & Information Technology, NED University of Engineering and Technology, Karachi, Pakistan
[3]Department of Artificial & Mathematical Sciences, Sindh Madressatul Islam University, Karachi, Pakistan

ABSTRACT The study and diagnosis of numerous skin disorders, including benign and malignant ones, have emerged as one of the central areas of research in the sphere of medical imaging. The advanced deep learning system known as Linear Sequential Convolutional Neural Networks (CNNs) has shown impressive abilities in automating image-related processes, including dermatological conditions and so on. This study explores how CNNs could be used to detect and classify the various skin disorders, including vitiligo, using the skin lesions dataset provided by Kaggle. This processing of images and data augmentation, and the use of ready-made models are the key elements of enhancing the system performance and generalization. This study proposes a robust Hybrid Model, designated as HGWO-GBPSO, which combines the exploratory power of the Grey Wolf Optimizer (GWO) with the refinement efficiency of Global Best Particle Swarm Optimization (GBPSO). The HGWO-GBPSO model exhibits an impressive accuracy and loss of 95.26, and 0.14 respectively. However, the average precision, recall, F1 score, and support.

INDEX TERMS deep learning, Grey Wolf Optimizer, medical image analysis, PSO, vitiligo classification

I. INTRODUCTION

Vitiligo is an autoimmune disorder, which involves the loss of skin pigmentation and is classified as a persistent and non-responsive skin disease [1]. Also, it poses a great cosmetic burden as it places a heavy psychosocial comorbidity on both the patients and their families [2]. As a result, the patients who have vitiligo usually show a wish to be treated, and have great expectations of early diagnosis and interventions [3]. Furthermore, dermoscopy is an easy and non-invasive method that examines pigmentary alterations in lesions at a sub- microscopic level [4]. Conversely, according to the dermoscopy images, manual dermatologist diagnosis is highly subjective and lacks reproducibility [5]. Nonetheless, Vitiligo dermatitis and stasis dermatitis are prevalent skin disorders that often pose difficulties in terms of diagnosis and evaluation. Hence, the analysis of skin images represents a valuable noninvasive method for the objective, automated, and quantitative evaluation of these dermatological issues [6]. At present, the development of the technologies that employ artificial intelligence (AI) in the

*Corresponding Author: shardhanand@ssuet.edu.pk

classification, diagnosis, and evaluation of clinical images of vitiligo is ongoing [7]. Nonetheless, prior research on the use of AI in vitiligo diagnosis has shown a comparatively poor level of evidence in populations, according to the specific clinical presentation, treatment approaches, and patient requirements in childhood vitiligo [8]. Additionally, deep learning and medical imaging have shown practical use in dermatology-related issues, including the analysis of vitiligo lesions of the face, offering valuable proofs toward the diagnosis of other dermatologic issues, including melanoma and cutaneous neoplasms [9]. Therefore, vitiligo diagnosis using dermoscopy images is inconsistent and subjective. Deep learning models have the capability to automatically identify and categorize depigmented areas on the skin and enhance precision, reproducibility and early diagnosis of skin cancer as opposed to conventional approaches [10]. Usually dermatologists use patch testing, blood tests, and biopsies to diagnose skin issues and recommend treatment. Yet, these treatments don't always work since they change a macule into a patch. To prevent treatment delays, many (ML) and (DL) models have been designed to identify macules early. Actually, researchers forecasted and classified vitiligo skin disease in normal skin with a DL-based model [11].

Vitiligo must be diagnosed accurately and promptly in order to respond to the disease. In line with this, the proposed study will improve vitiligo detection by incorporating a chaotic Grey Wolf Optimizer with CNNs, and by designing a hybrid HGWO-GBPSO alternative that would enhance the model robustness, accuracy, and optimization efficiency.

The following are the main objectives of this research.

- Integration of Grey Wolf Optimizer with CNN to enhance model robustness and precision.
- Mathematical integration and optimization of a chaotic Grey Wolf Optimizer with Particle Swarm Optimization, referred to as the Hybrid Grey Wolf Optimizer with Global Best PSO (HGWO-GBPSO). This hybrid approach leverages the leader-based exploration mechanism of GWO and the global best exploitation capability of PSO.

Evaluation of the proposed model in a heterogeneous environment to ensure robustness and generalization across diverse data distributions.

II. LITERATURE REVIEW

Usman *et al*. [12], presented a vitiligo diagnosis methodology based on the use of pre-processed dermatological images to train and compare a range of machine learning models. The essence of the strategy was two hybrid architectures that incorporated the InceptionV3 architecture with a CNN and a Random Forest classifier. These results showed that these proposed models had exceptional performance, showing perfect AUC scores of 1.0 and near perfect accuracies of 99.90% and 99.80, which are much better than all the models that were benchmarked.

Huang *et al*. [13] developed a deep learning hypopigmented dermatoses diagnosis and vitiligo severity evaluation system. A combination of a new composite severity indicator was used to classify the data with an SE_ResNet-18 model, and segment lesions with an HR-Net model. The findings showed the diagnostic model to perform highly with an accuracy of 0.9389, which was more accurate than 98 dermatologists, and the segmentation model had a mIOU of 0.8421. The suggested severity measure had medium clinical consistency, and it offered an automated and objective instrument to evaluate vitiligo.

Another paper introduces a complete framework of vitiligo segmentation of the body to allow clinical scoring directly. The methodology improves a baseline segmentation network with a custom-made contrast enhancement module, integrated successive dilation module to deal with long-range context, and a new confidence score refinement module that cross-checks the predictions of associated parts of the body. The algorithm was tested on the first standardized full-body vitiligo data of 1,740 images, with an average IoU of 0.8491 and a per-image error of 1.8. It scored better than an expert dermatologist on per-patient scoring accuracy, critically, and had a high likelihood of automated and objective clinical evaluation [14].

In another research, Reflectance Confocal Microscopy (RCM) was used to assess vitiligo stages on 217 patients who had three lesion sites namely, center, margin, and perilesional skin. A scoring system that was standardized was used to evaluate such features as pigment ring integrity and inflammation. Performance in terms of site dependence was found to differ: the lesion center presented high sensitivity (97.96) to detect progressive disease, and perilesional skin high specificity (90) to establish stability. Multi-site analysis was the most accurate in terms of overall (AUC 0.862), showing that a holistic approach to RCM provides the most predictable staging to be used as a clinical tool [15].

The current review investigates AI approaches to vitiligo management and focuses on the classification methods based on convolutional neural networks (CNNs) as ResNet and EfficientNet, and the lesion segmentation methods based on U-Net and YOLO. The reported results indicate high levels of performance with classification and segmentation accuracy rates of 97% and 97% respectively, even competing with clinician diagnosis. Nevertheless, there is still a limitation on the clinical translation of these tools due to a lack of validation on heterogeneous populations and integration issues. Their potential in standardizing diagnosis and monitoring should be developed in the future to focus on large-scale clinical trials, generalizability among skin types, and the ability to integrate the workflow to achieve value [16].

An automated approach for the detection of vitiligo was proposed in another research, based on a hybrid design; deep learning models (Inception v3, VGG19, VGG16), pre-trained for feature extraction from skin images, were combined with seven traditional machine learning models to classify the images. The best performance, 96.5% accuracy, was demonstrated with the combination of Inception v3 + Logistic Regression, thus offering an efficient diagnostic support tool for dermatologists [17].

In another study, ensemble CNN models on different color spaces were applied to support robust vitiligo classification by the probability averaging method, and AI and ML approaches were used to support early medical image-based diagnosis based on HOG feature extraction and PCA as the dimensionality reduction method, with optimized algorithms like GWO-ELM being efficient and effective in learning [18].

Guo *et al*. [19], established an innovative and hybrid AI model to impartially assess vitiligo marks on Asian patients with skin types III or IV disease. One after the other, this method utilized the UNet++ and YOLO v3 architectures to provide lesion classification, localization, and segmenting. For morphometric and colorimetric assessment of vitiligo lesions, three more parameters of area and color showed consistent results when compared with image analysis software and expert opinion from qualified dermatologists. The model was appropriate and could be applied in various clinical settings using only clinical images.

TABLE I

VITILIGO DEEP LEARNING BENCHMARKS (2023-2026)

Authors/Study	Year	Model/Algorithm	Dataset	Key Metrics	Research Gap
Frontiers AI review [20]	2025	EfficientNet-B7 (mobile app)	Clinical vitiligo images	Accuracy 95%	Needs larger multi-ethnic validation
ResNet/Swin Transformer [21]	2024	Optimized CNN/Transformer	Vitiligo clinical	High ACC, SEN, F1	Limited to binary diagnosis
Automated image analysis [22]	2025	DL-based segmentation	Dermosc-opy vitiligo	Improved JI/Dice	Real-time clinical integration
Hybrid IBGWO-PSO-RF [23]	2026	GWO-PSO + Random Forest	Skin lesion dataset	Enhanced feature selection	Vitiligo-specific tuning needed
Technological advances [19]	2025	Various AI (YOLO, UNet)	Mixed skin disease	Sensitivity ~90%	Diverse skin tone generalization

The existing AI, ML and DL based tools for the diagnosis of vitiligo have limitations in three major areas: dataset diversity, representation of features through pre-trained or single-modal models, and inadequate integration of existing tools. In this context, architectural enhancement of the model through Grey Wolf Optimization for facilitating feature learning and model generalization, and classification robustness of the CNN model is proposed in this work. In addition, hybrid chaotic GWO with global best PSO is used for optimizing convergence and accuracy in meeting the requirements for scalability and reliability in heterogeneous dermatological datasets.

III. METHODOLOGY

A. DATASET

The vitiligo dataset is taken from the Kaggle repository with total images of 3,628 containing two distinct classes (vitiligo, normal) in Figure 01. Furthermore, data augmentation is applied to the dataset in the second simulation to improve model robustness by increasing the number and diversity of images.

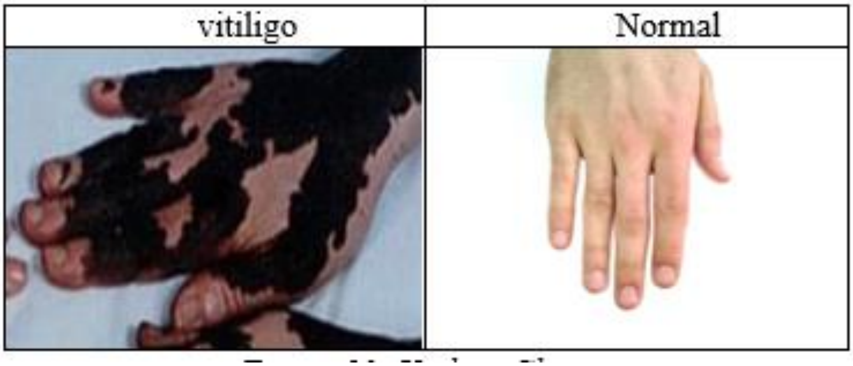

FIGURE 1. Vitiligo classes

B. IMAGE AUGMENTATION AND PRE PROCESSING

Image augmentation [24] is a method used to artificially expand a training dataset by applying realistic modifications to images, such as rotations, flips, or brightness adjustments. These transformations and image pre-processing (Fig1) help enhance model generalization and reduce the risk of over fitting.

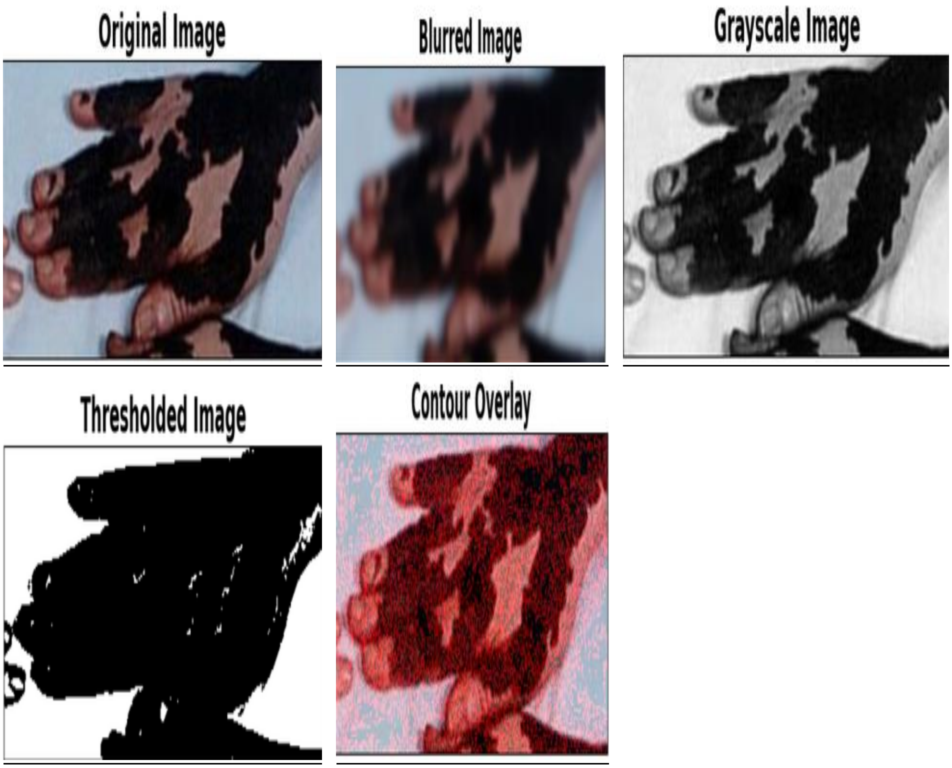

FIGURE 2. Image Pre-Processing

The mathematical equation for randomly rotating an image by ±15 degrees in image augmentation (Figure 2) is based on the affine transformation using a rotation matrix. The transformation can be expressed as in Eq. 01.

$$T = R(\theta) \cdot P \tag{1}$$

Where:

- $P = \begin{bmatrix} x \\ y \end{bmatrix}$ is the original pixel coordinate,
- $T = \begin{bmatrix} x' \\ y' \end{bmatrix}$ is the transformed coordinate,
- $R(\theta)$ is the rotation matrix, given Eq.2

$$R(\theta) = \begin{bmatrix} \cos\theta & -\sin\theta \\ \sin\theta & \cos\theta \end{bmatrix} \tag{2}$$

Where,

θ is randomly sampled from the range $[-15°, +15°]$ (or in radians: $\left[-\frac{\pi}{12}, +\frac{\pi}{12}\right]$).

Thus, the new pixel coordinates (x', y') After rotations are computed as:

$x' = x\cos\theta - y\sin\theta$ $y' = x\sin\theta + y\cos\theta$

This transformation is applied to all pixels in the image.

TABLE II
AUGMENTATION PARAMETERS

Parameter	Value	Effect
rescale	1.0/255	Normalizes pixel values from [0, 255] to [0, 1]
validation_split	0.3	Reserve 30% of data for validation.
rotation_range	15	Randomly rotates images by ±15 degrees
width_shift_range	0.2	Shifts width randomly by ±20% of the image width
height_shift_range	0.2	Shifts height randomly by ±20% of the image
zoom_range	0.2	Zooms in/out randomly by ±20% of the original
shear_range	0.1	Applies slight shear transformations (up to 10%
horizontal_flip	TRUE	Flips images horizontally (left-right) randomly.
fill_mode	'nearest'	Fills empty pixels after transforms using the nearest

TABLE III
OBJECTIVE FUNCTION HYPERPARAMETERS

Component	Parameters/Values	Description
Function Inputs	train_generator, val_generator	Training and validation data generators.
(Wolves/particles).	num_wolves=5	Number of search agents
Iterations	max_iter=10	Maximum optimization.
Search Space	dim=3	Dimensions: [filters, learning rate, dense units].
Bounds(Upper/lower)	[(16,64), (0.0001,0.01), (16,64)]	Ranges for filters, learning rate, and dense units.
Initialization	positions	Random positions within bounds (shape: num_wolves × dim).

Component	Parameters/Values	Description
	velocities	Zero-initialized velocities (shape: num_wolves × dim).
PSO Parameters	inertia=0.9, c1=1.5, c2=1.2	Controls velocity updates (exploration vs. exploitation).
Optimization Loop	for _ in range(10)	Runs for 10 iterations.
Update Rules	velocities[i] = ...	Updates velocity using PSO/GWO hybrid rules (blends social/cognitive terms).
	positions[i] += velocities[i]	Updates position with clipped bounds.
Termination	Returns alpha_pos, alpha_score	Best hyperparameters and their fitness score.

C. MODEL ROBUSTNESS

The robust model is considered to play a key role in model implementation and classification. To check model robustness, we have opted for two separate simulations to perform classification. The Hybrid Grey Wolf Optimizer with Global Best PSO (HGWO-GBPSO) blends the exploratory power of the GWO with the refinement efficiency of Global Best Particle Swarm Optimization (GBPSO). In this hybrid technique, GWO is enhanced to perform a global search by mimicking the social hierarchy and hunting behavior of grey wolves, whereas GBPSO is utilized to refine parameter solutions using the most efficient particles to increase convergence rates and accuracy. As a result, this hybrid technique combines the benefits of both techniques to create a perfect balance of exploration and exploitation, as demonstrated in Table 03, thus making it a highly efficient technique in solving complex optimization problems in machine learning.

D. GLOBAL BEST PARTICLE SWARM OPTIMIZATION

(GBPSO) is a variant of the conventional Particle Swarm Optimization (PSO) technique, which aims to enhance both the precision of solutions and speed of convergence. In GBPSO, a particle's update of position is based not only on the personal best solution of that particle but also on the global best solution among all particles in the swarm [25], [26]. The convergence of particles towards optimal solutions is possible in a more effective way by using a global communication mechanism, which decreases the chance of being trapped in local optima. GBPSO has been extensively used in a variety of domains, such as data science, engineering design, and machine learning, where effective optimization is essential, because of its capacity to strike a balance between exploration and exploitation [27]. The best position found within the entire swarm influences each particle in Global Best PSO (gBest PSO), where all particles share information globally.

The following are the mathematical formulas that control gBest PSO in equation Eq. 03.

1) VELOCITY UPDATE EQUATION (GLOBAL BEST PSO)

$$v_i^{(t+1)} = \omega v_i^{(t)} + c_1 r_1 \left(p_i^{(t)} - x_i^{(t)}\right) + c_2 r_2 \left(g^{(t)} - x_i^{(t)}\right) \tag{3}$$

Where,

$v_i^{(t+1)}$ is the updated velocity.

ω inertia weight controlling the influence of the previous velocity.

c_1 and c_2 are acceleration coefficients determining how much particles rely on their personal best ($p_i^{(t)}$) and global best ($g^{(t)}$) positions.

$r_1, r_2 \sim U(0,1)$ are random values sampled uniformly between 0 and 1.

$p_i^{(t)}$ is the personal best position

$g^{(t)}$ is the global best position

$x_i^{(t)}$ current position

2) POSITION UPDATE EQUATION

$$x_i^{(t+1)} = x_i^{(t)} + v_i^{(t+1)} \tag{4}$$

Where,

- $x_i^{(t+1)}$ new position of particle i.
- $v_i^{(t+1)}$ updated velocity

E. CHAOTIC MAP GREY WOLF

Developed to improve convergence speed and solution accuracy by including chaotic maps, the Chaotic Map Grey Wolf Optimizer (CMGWO) [28] is an improved variant of the conventional Grey Wolf Optimizer (GWO). GWO, inspired by nature, employs a metaheuristic approach that simulates the hunting and leadership strategies of grey wolves. Traditional GWO, however, can face challenges with early convergence and getting trapped in local optima. CMGWO incorporates chaotic graphs, such as logistics, tent, or sine maps, to introduce greater diversity and controlled randomness in the search process, addressing these limitations. By improving the balance between exploration and exploitation, it enhances search efficiency and overall optimization performance. CMGWO has proven effective across a wide range of real-world optimization problems, including energy management, machine learning, and engineering design.

1) MATHEMATICAL MODEL OF CMGWO

The mathematical foundation of CMGWO builds upon the original Grey Wolf Optimizer (GWO) while incorporating a chaotic map to enhance solution diversity.

The core equations of the standard GWO update the position of wolves as follows in Eq. 05:

$$\vec{D} = | \vec{C} \cdot \vec{X}_{\text{best}} - \vec{X} | \quad \vec{X}_{\text{new}} = \vec{X}_{\text{best}} - \vec{A} \cdot \vec{D} \tag{5}$$

Where:

$\vec{X}$ is grey wolf position.

$\vec{X}_{\text{best}}$ is the location of the best wolf (α, β, or δ).

$\vec{A}$ and $\vec{C}$ are constant vectors:

$\vec{A} = 2\vec{a} \cdot \vec{r}_1 - \vec{a}\, \vec{C} = 2 \cdot \vec{r}_2$

Where:

$\vec{a}$ linearly reducing control parameter.

$\vec{r}_1, \vec{r}_2$ are random vectors in [0,1].

2) INCORPORATING A CHAOTIC MAP

To improve exploration, a chaotic sequence $\chi(t)$ is used instead of a purely random number, such as Eq. 06.

$$\chi(t+1) = \mu\chi(t)\big(1 - \chi(t)\big) \tag{6}$$

where:

μ control parameter (often set to 4 in the logistic map).

$\chi(t)$ is the chaotic sequence at iteration t.

This chaotic sequence is then used to replace $\vec{r}_1$ or $\vec{r}_2$ in the standard Eq. 07.

$$\vec{A} = 2\vec{a} \cdot \chi(t) - \vec{a}\ \vec{C} = 2 \cdot \chi(t) \quad (7)$$

Thus, the updated position equation in CMGWO in Eq. 08:

$$\vec{X}_{new} = \vec{X}_{best} - (2\vec{a} \cdot \chi(t) - \vec{a}) \cdot | \vec{C} \cdot \vec{X}_{best} - \vec{X} | \quad (8)$$

The final hybrid position update equation in CMGWO-GBPSO is derived by integrating Equation (3) and Equation (5), where all components are unified into Equation (9).

$$x_i(t+1) = x_i(t) + w \cdot v_i(t) + c_1 \cdot r_1 \cdot \left(p_{best,i} - x_i(t)\right) + c_2 \cdot r_2 \cdot \left(g_{best} - x_i(t)\right) + \text{Chaotic Map} \cdot \left(A \cdot D_\alpha + B \cdot D_\beta + C \cdot D_\delta\right) \quad (9)$$

F. DEEP CONVOLUTIONAL NEURAL NETWORK

Under the umbrella of DL, CNN [29] is considered the most distinguished and widely used algorithm in this field. A key advantage of CNNs over earlier algorithms is their ability to autonomously identify important features without human intervention. CNNs are applied in a variety of domains, including image processing [30], audio analysis, and facial recognition, among others. Their structure is inspired by the neural architecture of human and animal brains and is similar to that of traditional neural networks.

1) FEATURE MAP IN CONVOLUTIONAL 2D

A fundamental process in CNNs that is vital for image feature extraction is Conv2D [31] (2D Convolution). It works by applying a trivial matrix, known as a kernel or filter, over an input image (or feature map) to identify patterns such as textures, edges and shapes. In this case, the Conv2D layer utilizes 32 filters, each measuring 3×3, along with the ReLU activation function and L2 regularization (λ=0.001). As mentioned in the equation ..., the ReLU function brings nonlinearity that aids the network in capturing complex patterns; L2 regularizations tend to discourage big weight values to lower overfitting.

The convolution operation (before activation) for the k-th filter is given in Eq. 10:

$$(X * W^k)_{i,j} = \sum_{m=0}^{2} \sum_{n=0}^{2} X_{i+m,j+n,1} \cdot W^k_{m,n,1} + b^k \quad (10)$$

Where

b^k is the bias term for the k-th filter.

2) RELU ACTIVATION

ReLU (Rectified Linear Unit) [32] activation is one of the most frequently used activation functions in neural networks, especially in deep learning. It is defined as in Eq 11.

$$A^k_{i,j} = \max\left(0, (X * W^k)_{i,j}\right) \quad (11)$$

where

A^k is the activation map for the k-th filter.

3) L2 REGULARIZATION

L2 regularization in machine learning also known as weight decay or Ridge Regression reduces over fitting by including a penalty term in the loss function. By reducing the sum of the square values of the model weights, this approach deters excessively heavy weight values and promotes a more balanced model. One can mathematically define the L2 regularized loss function as follows in Eq. 12:

$$\text{Loss} = \text{Original Loss} + \lambda * \Sigma w^2 \quad (12)$$

Where,

w stands for the model's weights and

The regularization parameter that defines the penalty's strength is (lambda) λ.

By avoiding needlessly big weights, L2 regularization enhances the model's generalizing ability and guarantees better performance on unobserved data. An extra regularization [33] term is now part of the loss function (Eq.13), where these regulatory terms are added.

The loss function's regularization term is:

$$\lambda \sum_{k=1}^{32} \sum_{m=0}^{2} \sum_{n=0}^{2} \left(W_{m,n,1}^{k}\right)^2 \quad (13)$$

where

$\lambda = 0.001.$

For each of the 32 output channels, the operation as shown in Eq. 14.

$$A^k = \mathrm{ReLU}(X * W^k + b^k), \text{for } k = 1, \dots, 32 \quad (14)$$

with the L2 regularization penalty combining eq 13 and 14 we get Eq.15. :

$$L_{\text{reg}} = 0.001 \cdot \sum_{k=1}^{32} \| W^k \|_F^2 \quad 15$$

where $\|\cdot\|_{\mathrm{F}}$ denotes the Frobenius norm [34] that quantifies a matrix's size or magnitude in a manner akin to that of the Euclidean norm, which quantifies a vector's length. Its definition is the sum of squared elements, which is the square root of the sum of the squares of every element in the matrix. The output tensor size is $62 \times 62 \times 32$, (assuming no padding, and stride = 1, since $64 - 3 + 1 = 62$).

G. THE MAXPOOLING2D

Max pooling [27] is a technique used in CNNs to gradually shrink the spatial dimensions (height x width) of feature maps while preserving the most significant information. It does this by moving a fixed-size window typically 2×2 across the input, and selecting the highest value from each region. This helps reduce computational complexity, improves feature extraction, and makes the model more robust to small variations in the input (2,2). Operation in Keras performs 2×2 max pooling with a stride of 2 (by default), meaning it selects the maximum value from each 2×2 non-overlapping window in the input feature map as mentioned below.

Given an input feature map $A \in R^{H \times W \times C}$,

Where:

H = height

W = width

C = number of channels

The output feature map $P \in R^{\frac{H}{2} \times \frac{W}{2} \times C}$ is computed in Eq. 16.

$$P_{i,j,c} = \max_{m=0}^{1} \max_{n=0}^{1} A_{2i+m, 2j+n, c} \quad (16)$$

where:

$i = 0, 1, \dots, \frac{H}{2} - 1$ (Rows in the pooled output)

$j = 0, 1, \dots, \frac{W}{2} - 1$ (Columns in the pooled output)

$c = 1, \dots, C$ (Channels remain unchanged)

H. DENSE KERNEL REGULARIZER

The Keras layer Dense presents a fully connected layer with 128 neurons, using the ReLU activation function and L2 regularization with a strength of 0.001. The regularization strength (lambda), which penalizes large weight values to prevent overfitting.

Let:

$x \in R^N$ be the input vector (with N features).

$W \in R^{N \times 128}$ be the weight matrix.

$b \in R^{128}$ be the bias vector.

$z \in R^{128}$ be the output before activation.

$y \in R^{128}$ be the final output after activation.

Compute the weighted sum in Eq.17.

$$z = Wx + b \tag{17}$$

Apply the Relu Activation Function in Eq.18.

$$y = \max(0, z) \tag{18}$$

Add L2 Regularization

The L2 regularization term is applied to the weight matrix W and is added to the loss function in Eq.19

$$L_{\text{reg}} = 0.001 \sum_{i=1}^{N} \sum_{j=1}^{128} W_{ij}^2 \tag{19}$$

I. SIGMOID

The Keras layer Dense (1, activation='sigmoid') represents a fully connected layer with a single neuron that applies the sigmoid activation function to its output. This is typically used in binary classification problems, where the output represents a probability between 0 and 1.

Let:

$x \in R^N$ be the input feature vector with N features.

$W \in R^N$ be the weight vector (since there is only 1 output neuron).

$b \in R$ be the bias term.

$z \in R$ be the weighted sum before activation.

$\boldsymbol{y} \in (\mathbf{0}, \mathbf{1})$ be the final output after applying the sigmoid activation function with compute the weighted sum in Eq.20

$$z = W^T x + b = \sum_{i=1}^{N} W_i x_i + b \tag{20}$$

This represents a dot product between the weight vector W and input vector x, plus the bias term b in Eq.21

$$y = \sigma(z) = \frac{1}{1+e^{-z}} \tag{21}$$

The sigmoid function [28] transforms z into a value between 0 and 1, making it suitable for binary classification into a final equation that describes how dense (1, activation='sigmoid') layer processes input and produces a probability output in Eq. 22.

$$y = \frac{1}{1 + e^{-(\sum_{i=1}^{N} W_i x_i + b)}} \tag{22}$$

IV. RESULT

The first simulation results show relatively strong classification performance with 92% overall accuracy. For class 0 (458 instances), the model achieved perfect recall (100%) and 84% precision, while class 1 (617 instances) showed perfect precision (100%) and 85% recall, with both classes having balanced F1-scores (91-92%). As shown in Table 04, the macro-averaged metrics (92–93%) and weighted averages (92–93%) indicate consistent performance across both classes despite a slight class imbalance. This demonstrates strong detection capabilities for both categories, with complementary strengths: class 0 identification minimizes false negatives, while class 1 predictions reduce false positives.

TABLE IV
ACCURACY METRICS (CLASSIFICATION REPORT)

Class	precision	recall	f1-score	support
0	0.84	1	0.91	458
1	1	0.85	0.92	617
Accuracy			0.92	1075
macro avg	0.92	0.93	0.92	1075
weighted avg	0.93	0.92	0.92	1075

Figure 3 shows that MobileNet coupled with the Grey Wolf Optimizer (GWO) has a good training accuracy of 94.5% and a consistent validation peak of 89.5% across 12 epochs. The GWO is a successful model tuner that enables the lightweight MobileNet architecture to learn complicated patterns with a healthy generalization gap. The fact that it is on an upward trend and has no trend line is a testament to the stability of the system and its capability to work with unknown data with reasonable accuracy.

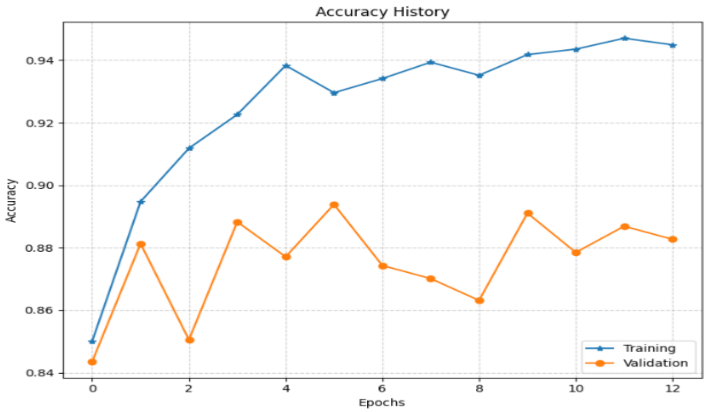

FIGURE 3. Training curves (mobile net + grey wolf)

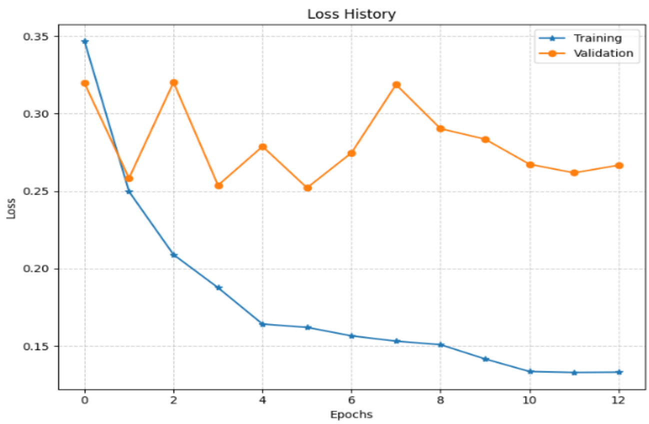

FIGURE 4. Training loss(mobile net + grey wolf)

Figure 4 demonstrates that MobileNet-GWO model has an efficient convergence with a training loss of 0.13 and validation loss range of 0.25-0.32. The fact that the first peak reduced sharply highlights that the Grey Wolf Optimizer is effectively able to find the optimal weights, and the overall decreasing trend of eight epochs proves the stability and generalization of the system.

ROC is steady enough with no such deflection for error rate. ROC in figure 05 shows a steady enough graph with no deflection for error rate whatsoever. A confusion matrix is a valuable tool for estimating the performance of a classification model by displaying the number of correct and incorrect predictions for each class. In this matrix, the model correctly predicted 573 cases as 1 (True Positives) and 458 cases as 0 (True Negatives). Additionally, there were no False Positives (FP = 0), meaning the model never mistakenly classified a 0 as a 1. However, there were 44 False Negatives, where the model incorrectly predicted 0 instead of 1. This results in an overall accuracy of 95.91%, indicating strong model performance. The precision, which measures how often the model's positive predictions were correct, is 100%, showing that every predicted 1 was indeed a 1 as mentioned in Figure 06.

A. HISTOGRAM

This histogram displays the distribution of predicted probabilities from a classification model as shown in figure 07. The distribution appears bimodal, with peaks near 0.1 and 0.8, indicating that the model confidently predicts most cases as either low probability (closer to 0) or high probability (closer to 1). This suggests the model is making strong classifications with few uncertain predictions near 0.5, which is ideal for a well-calibrated classifier.

B. HGWO-GBPSO CLASSIFICATION

Figure 8 and Figure 9 display that MobileNet + Grey wolf + PSO hybrid model has good convergence, reaching training accuracy of approximately 94%, and validation of 88% by epoch 7 with insignificant overfitting. The loss on training decreases to 0.30 to approximately 0.15, and validation loss also decreases from 0.34 to approximately 0.24, as a sign of successful hybrid optimization and good generalization in the case of vitiligo classification. For the "healthy" class, the model had a precision of 95.71%, a recall of 97.59% , and an F1-score of 96.64, based on HGWO-GBPSO 458 samples. For the vitiligo class, it achieved 98.19% precision, 96.75% recall, and an F1-score of 97.46, with 617 samples. The macro average, which treats both classes equally, resulted in a precision of 96.95%, a recall of 97.17%, and an F1-score of 97.05%. Meanwhile, the weighted average, which accounts for class imbalance, showed 97.13% precision, 97.11% recall, and an F1-score of 97.11%, based on a total of 1,075 samples. These metrics indicate that the model performs well across both classes, with high precision and recall, ensuring minimal misclassifications.

TABLE V

MACRO AND WEIGHTED AVERAGE

Healthy	Vitiligo
precision: 95.71	precision: 98.19
recall: 97.59	recall: 96.75
f1-score: 96.64	f1-score: 97.46
support: 458.0	support: 617.0
accuracy: 97.11	
macro avg	weighted avg
precision: 96.95	precision: 97.13
recall: 97.17	Recall: 97.11
f1-score: 97.05	f1-score: 97.11
support: 1075.0	support: 1075.0

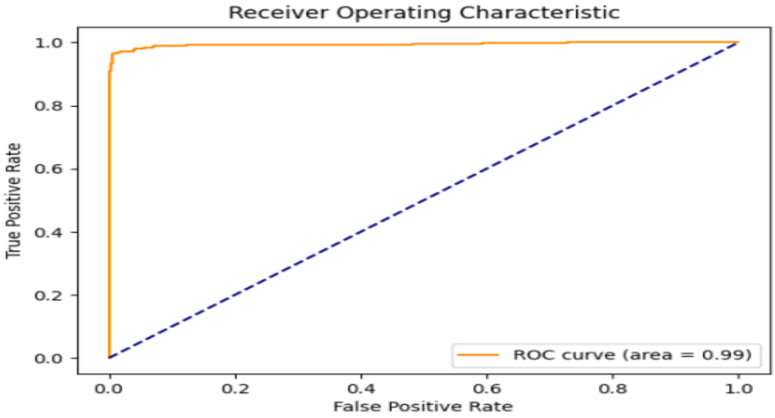

FIGURE 5. ROC curve

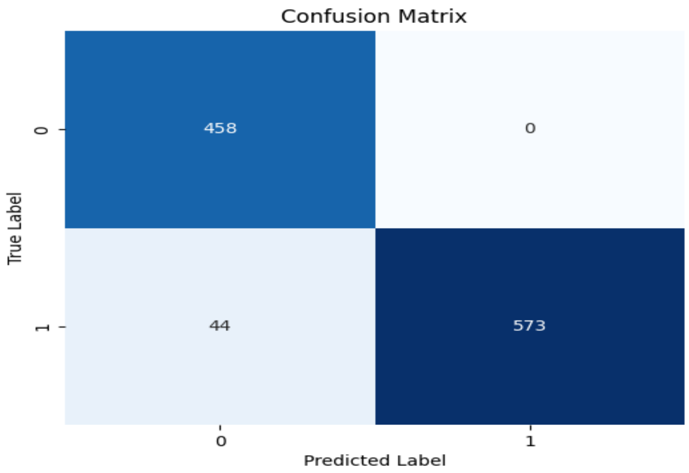

FIGURE 6. Confusion matrix

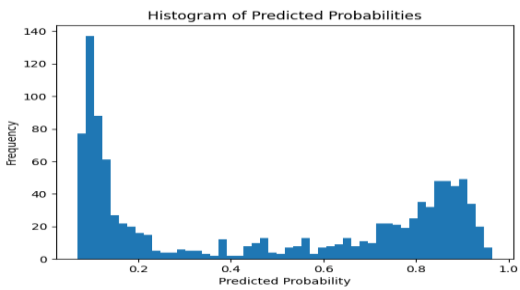

FIGURE 7. Histogram

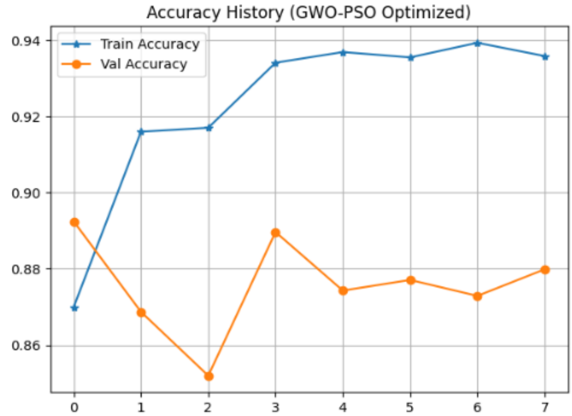

FIGURE 8. Training curves (mobilenet+grey wolf + PSO)

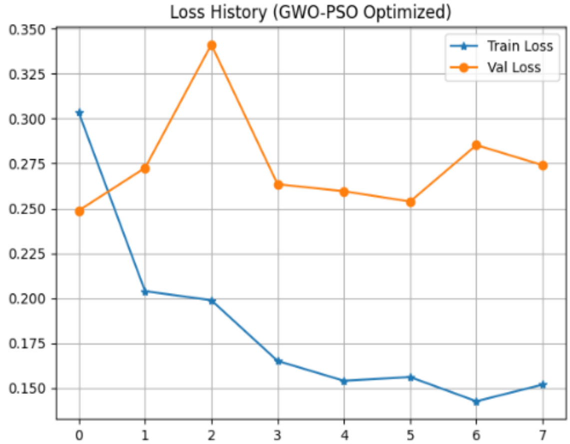

FIGURE 9. Training Loss (mobilenet+grey wolf + PSO)

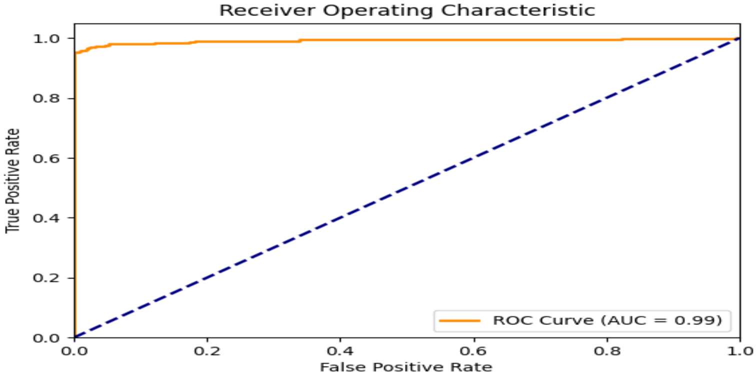

FIGURE 10. ROC-AUC curves

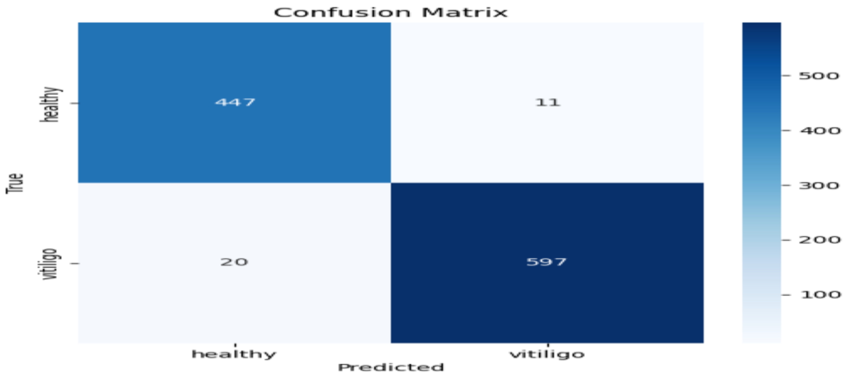

FIGURE 11. Confusion matrix

V. CONCLUSION

The present study introduces an optimized deep learning framework for automatic classification of vitiligo by combining a linear sequential CNN with a hybrid HGWO-GBPSO optimization strategy. The proposed model presents an efficient balance between exploration and exploitation by combining the capability of the Grey Wolf Optimizer in global exploration with the fast convergence capability of Global Best Particle Swarm Optimization. Experimental results from the Kaggle vitiligo dataset illustrate that the HGWO-GBPSO model outperforms baseline approaches, with high accuracy, low loss, and robustness in the precision-recall performance for both classes. The reliable ROC characteristics and low misclassification rates further establish the credibility of the proposed approach. This work, thus, underlines the efficiency of hybrid metaheuristic optimization in improving CNN-driven medical image analysis and provides a promising direction for objective and automated diagnosis of vitiligo in clinical applications.

A. FUTURE WORK

Particle Swarm Optimization (PSO) may solve the Actor-Critic problem in reinforcement learning in the future by improving the Actor-Critic by dynamically altering parameters during the training phase, thereby enabling the investigation of a wider range of generated samples.

Author Contribution

Shardha Nand: conceptualization, methodology, data analysis, software development, writing – original draft, writing – review & editing. **Asif Raza:** data collection. **Usman Amjad:** supervision**. Nancy Alias Shivani Kumari:** writing – original draft, validation, visualization.

Conflict of Interest

The authors of the manuscript have no financial or non-financial conflict of interest in the subject matter or materials discussed in this manuscript.

Data Availability Statement

Data supporting the findings of this study will be made available by the corresponding author upon request.

Funding Details

No funding has been received for this research.

Generative AI Disclosure Statement

The authors did not use any type of generative artificial intelligence software for this research.

REFERENCES

[1] S. Yu, Z. Chen, J. He, and H. Wang, "Comparative study of dermatologists and deep learning model on diagnosing childhood vitiligo," *Photodiagn. Photodyn. Ther.*, vol. 54, Aug. 2025, Art. no. 104727, doi: https://doi.org/10.1016/j.pdpdt.2025.104727.

[2] M. Böhm, R. Sommer, U. Gieler, P. Staubach, A. Zink, C. Apfelbacher, *et al.*, "Vitiligo–a disease: A position paper on stigmatization, life quality impairment and psychosocial comorbidity," *JDDG: J. der Deutschen Dermatol. Gesells.*, vol. 22, pp. 1327–1335, 2024, doi: https://doi.org/10.1111/ddg.15503.

[3] I. H. Hamzavi, K. Bibeau, P. Grimes, J. E. Harris, N. van Geel, D. Parsad, *et al.*, "Exploring the natural and treatment history of vitiligo: Perceptions of patients and healthcare professionals from the global VALIANT study," *Br. J. Dermatol.*, vol. 189, pp. 569–577, Nov. 2023, doi: https://doi.org/10.1093/bjd/ljad245.

[4] S. Hayes, "Dermoscopy: the dermatologist's stethoscope," *Clin. Experiment. Dermatol.*, vol. 49, no. 9, June 2024, Art. no. 955, doi: https://doi.org/10.1093/ced/llae241.

[5] S. Ye and M. Chen, "The emerging role of artificial intelligence in diagnosis and clinical analysis of dermatology," *Dermatol. Sin.*, vol. 41, pp. 145–152, 2023, doi: https://doi.org/10.4103/ds.DS-D-23-00025.

[6] A. Kallipolitis et al., "Skin image analysis for detection and quantitative assessment of dermatitis, vitiligo and alopecia areata lesions: A systematic literature review," *BMC Med. Inform. Decis. Mak.*, vol. 25, Jan. 2025, doi: https://doi.org/10.1186/s12911-024-02843-2.

[7] J. A. Godínez-Chaparro, R. Roldán-Marín, H. Vidaurri-de la Cruz, L. A. Soto-Mota, and K. Férez, "Dermatoscopic patterns in vitiligo," *Dermatol. Pract. Concept.*, vol. 13, Oct. 2023, Art. no. 2023197, doi: https://doi.org/10.5826/dpc.1304a197.

[8] P. Abdi et al., "Non-invasive skin measurement methods and diagnostics for vitiligo: A systematic review," *Front. Med.*, vol. 10, July 2023, Art. no. 1200963, doi: https://doi.org/10.3389/fmed.2023.1200963.

[9] M. M. Hasan, J. Phu, A. Sowmya, E. Meijering, and M. Kalloniatis, "Artificial intelligence in the diagnosis of glaucoma and neurodegenerative diseases," *Clin. Exp. Optom.*, vol. 107, pp. 130–146, 2024, doi: https://doi.org/10.1080/08164622.2023.2235346.

[10] J. Zhang, F. Zhong, K. He, M. Ji, S. Li, and C. Li, "Recent advancements and perspectives in the diagnosis of skin diseases using machine learning and deep learning: A review," *Diagnostics*, vol. 13, Nov. 2023, Art. no. 3506, doi: https://doi.org/10.3390/diagnostics13233506.

[11] S. Sharma, K. Guleria, S. Kumar, and S. Tiwari, "Deep learning-based model for detection of vitiligo skin disease using pre-trained Inception V3," *Int. J. Math. Eng. Manag. Sci.*, vol. 8, 2023, Art. no. 1024, doi: https://doi.org/10.33889/IJMEMS.2023.8.5.059.

[12] M. Usman, M. Y. Iqbal, K. Zafar, and S. Basharat, "A novel approach to vitiligo diagnosis using artificial neural networks and dermatological image analysis," *J. Comput. Biomed. Inform.*,

vol. 8, no. 1, 2024, Art. no. 736-0801/2024.

[13] H. Huang et al., "Intelligent diagnosis of hypopigmented dermatoses and intelligent evaluation of vitiligo severity on the basis of deep learning," *Dermatol. Ther.*, vol. 14, pp. 3307–3320, Nov. 2024, doi: https://doi.org/10.1007/s13555-024-01296-9.

[14] Y. Li, S. T. G. Thng, and A. W.-K. Kong, "Bridging the gap between vitiligo segmentation and clinical scores," *IEEE J. Biomed. Health Inform.*, vol. 28, pp. 1623–1634, 2023, doi:https://doi.org/10.1109/JBHI.2023.3342069.

[15] J. Wu, M. Sun, Z. Wei, Q. Jiang, H. Chen, and L. Chen, "Sensitivity and specificity analysis of different lesion areas of vitiligo by reflectance confocal microscopy," *J. Cosmet. Dermatol.*, vol. 24, 2025, Art. no. 70006, doi: https://doi.org/10.1111/jocd.70006.

[16] M. Parikh, G. Fang, F. Poon, M. Kyeremeh, D. Cruz, K. Ki, *et al.*, "Technological advances in vitiligo management: Perspectives on AI, mobile tools, and clinical utility," *Front. Med.*, vol. 12, 2025, doi: https://doi.org/10.3389/fmed.2025.1661554.

[17] M. Z. Hussain, M. Z. Hasan, M. M. Baig, T. Khan, S. Nosheen, A. M. Bhatti, *et al.*, "Malware/ransomware analysis and detection," in *Proc. WorldS4 Conf.*, 2023, pp. 339–352, doi: https://doi.org/10.1007/978-981-99-8031-4_30.

[18] Q. Shi-fan, T. Jun-kun, Z. Yong-gang, W. Li-jun, Z. Ming-fei, T. Jun, *et al.*, "Settlement prediction of foundation pit excavation based on the GWO-ELM model," *Adv. Civ. Eng.*, vol. 2021, 2021, doi: https://doi.org/10.1155/2021/8896210.

[19] L. Guo, Y. Yang, H. Ding, H. Zheng, H. Yang, J. Xie, *et al.*, "A deep learning-based hybrid artificial intelligence model for vitiligo detection and severity assessment," *Ann. Transl. Med.*, vol. 10, May 2022, Art. no. 590, doi: https://doi.org/10.21037/atm-22-1738.

[20] M. Parikh, G. Fang, F. Poon, M. Kyeremeh, D. Cruz, K. Ki, *et al.*, "Technological advances in vitiligo management: Perspectives on AI, mobile tools, and clinical utility," *Front. Med.*, vol. 12, Oct. 2025, doi: https://doi.org/10.3389/fmed.2025.1661554.

[21] F. Zhong, "Optimizing vitiligo diagnosis with ResNet and Swin transformer deep learning models," *Sci. Rep.*, vol. 14, 2024, Art. no. 9127, doi: https://doi.org/10.1038/s41598-024-59436-2.

[22] R. Mazzetto, A. Sernicola, J. Tartaglia, C. Ciolfi, and M. Alaibac, "Potential of automated image analysis for the measurement of vitiligo lesions," *Front. Med.*, vol. 12, 2025, doi: https://doi.org/10.3389/fmed.2025.1623408.

[23] A. Al Abdulwahid, S. S. Alqahtany, D. Syed, M. S. Al Reshan, K. Rajab, and A. Shaikh, "A hybrid improved binary GWO-PSO with random forest-based intrusion detection model," *Sci. Rep.*, 2026, doi: https://doi.org/10.1038/s41598-025-33242-w.

[24] M. Xu, S. Yoon, A. Fuentes, and D. S. Park, "A comprehensive survey of image augmentation techniques for deep learning," *Pattern Recognit.*, vol.

137, Art. no. 109347, 2023.

[25] L. Kumar, M. Pandey, and M. K. Ahirwal, “Parallel global best-worst particle swarm optimization algorithm,” *Appl. Soft Comput.*, vol. 142, July 2023, Art. no. 110329, doi: https://doi.org/10.1016/j.asoc.2023.110329.

[26] F. Chen, X. Sun, D. Wei, and Y. Tang, “Tradeoff strategy between exploration and exploitation for PSO,” in *Proc. Int. Conf. Nat. Comput.*, 2011, pp. 1216–1222.

[27] Z. Xu, H. Yang, J. Li, X. Zhang, B. Lu, and S. Gao, “Comparative study on chaotic grey wolf optimization algorithms,” *IEEE Access*, vol. 9, pp. 77416–77437, 2021, doi: https://doi.org/10.1109/ACCESS.2021.3083220.

[28] L. Alzubaidi *et al.*, “Review of deep learning: concepts, CNN architectures, challenges, applications, future directions,” *J. Big Data*, vol. 8, pp. 1–74, Mar. 2021, doi: https://doi.org/10.1186/s40537-021-00444-8.

[29] P. Das and D. H. Mazumder, “MLCNNF: A multi-label CNN framework for predicting adverse COVID drug reactions,” *IEEE Trans. Comput. Biol. Bioinform.*, 2025, doi: https://doi.org/10.1109/TCBBIO.2024.3515480.

[30] G. Averkov, C. Hojny, and M. Merkert, “On the expressiveness of rational ReLU neural networks,” *arXiv*, 2025. [Online]. Available: https://doi.org/10.48550/arXiv.2502.06283.

[31] Y. Zhao, X. Deng, J. Zhang, and P. Wang, “Spatio-temporal regularized stochastic configuration network,” *IEEE Trans. Autom. Sci. Eng.*, vol. 22, Jan. 2025, doi: https://doi.org/10.1109/TASE.2025.3531850.

[32] Y. Guo, G. Chen, T. Zeng, Q. Jin, and M. K.-P. Ng, “Quaternion nuclear norm minus Frobenius norm minimization,” *Pattern Recognit.*, vol. 158, Feb. 2025, Art. no. 110986, doi: https://doi.org/10.1016/j.patcog.2024.110986.

[33] G. Ekambaram and T. Rakkiannan, “Transfer learning-based deep learning model for facial expression,” in *Proc. IEEE IDCIoT*, 2025, pp. 2030–2037, doi: https://doi.org/10.1109/IDCIOT64235.2025.10915054.

[34] D. Yu and F. Cao, “Construction and approximation rate for feedforward neural network operators,” *J. Comput. Appl. Math.*, vol. 453, Jan. 2025, Art. no. 116150, doi: https://doi.org/10.1016/j.cam.2024.116150.